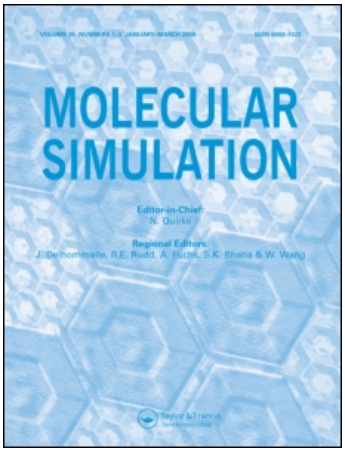

Molecular Simulation
Publication details, including instructions for authors and subscription information:
http://www.informaworld.com/smpp/title~content=t713644482

Quantum transport in nano MOSFETs

V. J. Lamba[a]; Derick Engles[b]; S. S. Malik[c]; A. Gupta[d]
[a] Department of ECE, HCTM, Kaithal, India [b] Department of ECE, GND University, Amritsar, India [c] Department of Physics, GND University, Amritsar, India [d] Department of EEE, HCTM, Kaithal, India

To cite this Article Lamba, V. J. , Engles, Derick , Malik, S. S. and Gupta, A.(2009) 'Quantum transport in nano MOSFETs', Molecular Simulation, 35: 6, 434 — 439
To link to this Article: DOI: 10.1080/08927020802512211
URL: http://dx.doi.org/10.1080/08927020802512211

Molecular Simulation
Vol. 35, No. 6, May 2009, 434–439

Taylor & Francis
Taylor & Francis Group

Quantum transport in nano MOSFETs

V.J. Lamba[a]*, Derick Engles[b], S.S. Malik[c] and A. Gupta[d]

[a]*Department of ECE, HCTM, Kaithal, India;* [b]*Department of ECE, GND University, Amritsar, India;* [c]*Department of Physics, GND University, Amritsar, India;* [d]*Department of EEE, HCTM, Kaithal, India*

(*Received 5 September 2008; final version received 27 September 2008*)

In this work, a general method for describing quantum electron transport will be introduced. These formulations are based on Schrödinger equation, Pauli master equation, density matrix, Wigner function and the Green function. Here, we describe the microscopic quantum theory of electron transport in silicon devices based on the NEGF formalism. We review the NEGF formalism and derive its key equations. We include the electron–phonon interactions and other scattering mechanisms such as the impurity scattering and the surface roughness scattering. For the electron–electron interactions, we used the assumption that each electron moves independently and sees only the average field generated by all the other electrons.

Keywords: length scale; Green's function; scattering; broadening; mobility

1. Introduction

Various quantum mechanical formulations have been used for the modelling of the carrier transport in semiconductor devices. During the 1980s, advances in the semiconductor technology made it possible to fabricate conductors so small that the quantum nature of electrons could be directly observed in transport experiments. A typical system used for these studies includes quantum dots [1] and point contacts [2], which are formed by manipulating the electrostatic potential in a two-dimensional electron gas by means of gate electrodes. The size of these semiconductor structures is of the order of micrometres, which characterises them as mesoscopic systems, intermediate between the microscopic and macroscopic. Several important discoveries such as the quantum Hall effect and quantisation of conductance are all results of the intense study of electron transport [3].

The paper is organised as follows. In Section 2, we start with an introduction of length scales, used to characterise electron transport. Section 3 describes the Hamiltonian of a system. Section 4 includes the Green function and study of properties of kinetic equations. The electron–phonon interactions and other scattering mechanisms (including surface roughness scattering) will be included in Section 5, and a simple nano MOSFET will be discussed.

2. Length scales

A key quantity in the description of electron transport is the electrical conductance relating the current through a conductor to the applied voltage. For a macroscopic sample, the conductance is given by

$$G = \sigma \frac{A}{L}, \tag{1}$$

where A and L are the cross-sectional area and the length of the sample, respectively, and σ is the material-dependent conductivity. When the dimensions of the sample become sufficiently small the quantum nature of the charge carriers becomes important, and the classical relation (1) breaks down. Below we introduce three length scales that are important in microscopic description of electron transport.

2.1 Fermi wavelength

The wave function of an electron in a crystalline metal contains a Bloch factor, exp(ik **r**), which determines the complex phase of the wave function throughout the crystal [4]. The wavelength of this oscillating phase associated with a conduction electron at the Fermi level is called the Fermi wavelength, $\lambda_F = 2\pi/k_F$. In semiconductors the density of conduction electrons is very low, which can be several nanometres.

2.2 Phase coherence length

The phase coherence time, τ_φ, is the time during which the phase of an electron is completely lost due to interactions with the dynamic environment. The dynamic environment consists of all quantum degrees of freedom, which interact

*Corresponding author. Email: lamba_vj@hotmail.com

ISSN 0892-7022 print/ISSN 1029-0435 online

DOI: 10.1080/08927020802512211
http://www.informaworld.com

with the electron such as phonons, impurities and the other conduction electrons. The phase coherence length, l_φ, is defined as the distance a conduction electron moves before its phase is lost, i.e. $l_\varphi = \upsilon_F\, \tau_\varphi$.

2.3 *Mean free path*

The mean free path is defined from the momentum relaxation time, τ_m, which is the time it takes for a conduction electron to lose its initial momentum through scattering events. In a perfect crystal the electron moves unhindered, and thus $\tau_m = \infty$. In a real system, however, the presence of scatterers will reduce τ_m to a finite value. It should be noted that the scattering events relaxing the momentum can be elastic as well as inelastic and thus there is no *a priori* relation between τ_m and τ_φ.

The relative size of the length scales introduced above defines, in combination with the characteristic system dimension, L, various different transport regimes. The systems considered in the present work is assumed to be in the phase-coherent regime, where $l_\varphi > L$. These systems are large compared to the atomic scale, and the large λ_F characteristic for these systems renders the electrons insensitive to the detailed atomic structure of the host material. This, of course, simplifies some aspects of the theoretical modelling of transport in semiconductor systems.

3. Hamiltonian of system

Let us consider an isolated device and its energy levels, described using a Hamiltonian H, a Hartree potential U and energy eigenstates of the electron ε_α,

$$(H + U)\psi_\alpha(\vec{r}) = \varepsilon_\alpha \psi_\alpha(\vec{r}). \tag{2}$$

The Hamiltonian of the considered system, H, is composed of four different components as

$$H = H_e + H_p + H_{e-p} + H_{is} \tag{3}$$

where H_e is the Hamiltonian of non-interacting electrons, H_p is the Hamiltonian of free phonons, H_{e-p} is the electron–phonon interaction Hamiltonian and H_{is} is the Hamiltonian for impurity scattering. In this section, we introduce these components one by one.

3.1 *Hamiltonian of non-interacting electrons*

As we use the Hartree approximation to simplify the electron–electron interaction, the Hamiltonian of non-interacting electrons can be written as [5]

$$H_e = \int \mathrm{d}r \psi^\dagger(\vec{r}) \left[T(\vec{r}) + U(\vec{r})\right] \psi(\vec{r}), \tag{4}$$

where $T(\vec{r})$ is one-electron K.E and $U(\vec{r})$ is self-consistent electrostatic P.E. operator. The expression for the one-electron kinetic energy operator is obtained from the effective mass approximation. Since we consider the transport of electrons in the conduction band of silicon, we use the usual parabolic, ellipsoidal energy band structure, which is found to be a reasonable approximation even in the nanoscale devices [6].

3.2 *Hamiltonian of free phonons*

The Hamiltonian of free phonons can be written as [7]

$$H_p = \sum_{\mathbf{q}\lambda} \hbar\omega_{\mathbf{q}\lambda} \left(a^\dagger_{\mathbf{q}\lambda} a_{\mathbf{q}\lambda} + \frac{1}{2} \right), \tag{5}$$

where $\omega_{\mathbf{q}\lambda}, a^\dagger_{\mathbf{q}\lambda}$, and $a_{\mathbf{q}\lambda}$ are the angular frequency, the creation operator and the annihilation operator for mode λ and wavevector $\mathbf{q}$, respectively.

3.3 *Electron–phonon interaction Hamiltonian*

In the first quantisation picture, the electron–phonon interaction Hamiltonian felt by the electrons in the conduction band can be obtained from the deformation potential theory as [8]. As in the continuous medium approximation, the ion displacement field y can be written in terms of the phonon creation and annihilation operators. Thus, we obtain the single-electron interaction Hamiltonian in terms of the phonon creation and annihilation operators as

$$\varphi(\vec{r}) = \frac{1}{\sqrt{V}} \sum_{\mathbf{q}\lambda} M_{\mathbf{q}\lambda} \left[a_{\mathbf{q}\lambda} + a^\dagger_{-\mathbf{q}\lambda} \right] \mathrm{e}^{i\mathbf{q}.\vec{r}}, \tag{6}$$

where the electron–phonon matrix element $M_{\mathbf{q}\lambda}$ is

$$M_{\mathbf{q}\lambda}(\vec{r}) = i \left(\frac{\hbar}{2\rho V \omega_{\mathbf{q}\lambda}} \right)^{1/2} \sum_{i=1}^{3} \sum_{j=1}^{3} \Xi_{lj} \mathbf{q}_l \xi_{j\lambda}, \tag{7}$$

which has the following property: $M_{-\mathbf{q}\lambda} = M^*_{\mathbf{q}\lambda}$. From the obtained single-electron operator for the electron–phonon interaction Hamiltonian (6), we obtain the second quantised electron–phonon interaction Hamiltonian as

$$H_{e-p} = \int \mathrm{d}r \psi^\dagger(\vec{r}) \psi(\vec{r}) \varphi(\vec{r}). \tag{8}$$

3.4 *Hamiltonian for impurity scattering [7]*

Impurity scattering is an interaction between a moving carrier and a fixed ionised atom. Its Hamiltonian is

given by

$$H_{\text{is}} = \sum_i \int \mathrm{d}r\psi^{\dagger}(\vec{r})V\left(\vec{r} - \vec{R}_i\right)\hat{\psi}(\vec{r}), \tag{9}$$

where $\hat{\psi}^{\dagger}$and$\hat{\psi}$ are creation and annihilation operators, and $V(\vec{r} - \vec{R}_i)$ is the potential describing the interaction between a carrier at site **r** and an impurity at site $\mathbf{R}_i$.

4. Green's function

Here, the main equations governing the behaviour of non-equilibrium Green's functions are presented as well as the derivation of two important physical quantities resulting from their solution, the carrier density and the current density. The total Hamiltonian $H(t)$ of system is given by

$$H(t) = H + H_{\text{ext}}(t) = H_0 + V + H_{\text{ext}}(t), \tag{10}$$

where H_0 is the non-interacting part of the Hamiltonian, V contains all the interactions (carrier–carrier, carrier–phonon, impurity scattering, etc) and $H_{\text{ext}}(t)$ is an external perturbation driving the system out of equilibrium. Thus,

$$H_{\text{ext}}(t) = \int \mathrm{d}x\psi^{\dagger}(x)U(x,t)\psi(x). \tag{11}$$

Here, $U(x,t)$ is the external potential. In general, an isolated device and its energy levels are described using a Hamiltonian H, a Hartree potential U and energy eigenstates of the electron, ε_α by (2) and its Hamiltonian by (3). In general, the electron density matrix in real space is given by

$$\left[\rho(\vec{r},\vec{r}';E)\right] = \int_{-\infty}^{+\infty} f(E - E_f)\,\delta([EI - H])\mathrm{d}E. \tag{12}$$

Here, $\delta(EI - H)$ is the local density of states, rewriting further using the standard expansion form Equation (12) become

$$\delta(EI - H) = \frac{i}{2\pi}\Big(\left[G(E) - G^{+}(E)\right] \text{ where } G(E) = \left[(E - i0^{+})I - H\right]^{-1}\Big),$$

where $G(E)$ is the retarded Green's function, while $G^{+}(E)$, its conjugate complex transpose, is called the advanced Green function. In the time domain, the Green function can be interpreted as the impulse response of the Schrödinger equation, where, in the present scenario, the impulse is essentially an incoming electron at a particular energy. In the energy domain, the Green function gives the energy eigenvalues for the eigenstates that are occupied in response to the applied impulse. As the electron density in the channel is the product of the Fermi function and the available density of states, so for an isolated device it is written as

$$\rho(\vec{r},\vec{r}';E) = \int_{-\infty}^{+\infty} f(E - E_f)[A(E)]\frac{\mathrm{d}E}{2\pi}. \tag{13}$$

The real portion of the diagonal elements of the density matrix represents the electron density distribution in the channel. To understand the process of current flow, consider an isolated device having a single energy level ε. The source and drain contacts have an infinite distribution of electronic energy states. When the isolated device with single energy level ε is connected to the source and drain contacts, some of the density of states around this energy level ε will spill over from the contacts into the channel. This process is known as energy level *broadening*. If the Fermi levels in the source and drain are equal, the amount of broadening will be equal on both sides and hence the net current flow in the channel will be zero. When a positive bias is applied on the drain side, the Fermi level on the drain side is lowered according to Equation (14), opening up states below the channel energy level ε in the drain,

$$E_{f_2} = E_{f_1} - qV_D. \tag{14}$$

The electrons entering the channel with energy ε now have states with lower energies available in the drain to escape to. This causes the channel current to become non-zero. As the applied bias is increased linearly, more and more states between ε and ε_{f_2} become available to remove electrons from the channel causing the source to increase its supply of electrons into the channel. This phenomenon results in a linear increase of current in the channel. Eventually, the difference in the channel energy level ε and the drain Fermi level ε_{f_2} is so great that there are no additional states around the energy ε in the drain for the channel electrons to escape. The current reaches saturation such that the number of electrons leaving the drain will equal the number of electrons entering from the source. This process also explains why experimental measurements [9] have shown that the maximum measured conductance of a one-energy level channel approaches a limiting value $G_0 = 2q^2/\hbar = 51.6\,\mathrm{K}\Omega^{-1}$.The above analogy of a one-energy level system is applicable to nanoscale thin films and wires, where available energy levels along the confined dimension are very limited in addition to being spaced far apart from adjacent energy levels.

In the NEGF formalism, the coupling of the device to the source and drain contacts is described using self-energy matrices, Σ_1 and Σ_2. The self-energy term can be viewed as a modification to the Hamiltonian to incorporate the boundary conditions. Accordingly, Equation (2) and (12)

can be rewritten as

$$\left(H + U + \sum\nolimits_1 + \sum\nolimits_2\right)\psi_\alpha(\vec{r}) = \varepsilon_\alpha \psi_\alpha(\vec{r}). \tag{15}$$

The self-energy terms Σ_1 and Σ_2 originate from the solution of the contact Hamiltonian. In this semi-infinite system, which is connected to the channel, there will be an incident wave from the channel as well as a reflected wave from the contact. The wave function at the interface is matched to conserve energy resulting in the boundary condition,

$$\sum\nolimits_j = -t\exp\left(ik_j a\right), \tag{16}$$

where, t the inter-unit coupling energy resulting from the discretisation is given by

$$t = \frac{\hbar^2}{2m^* a^2}. \tag{17}$$

Here, k_j corresponds to wavevector of the electron entering from the channel while a corresponds to the grid spacing. The broadening of the energy levels introduced by connecting the device to the source and drain contacts is incorporated through gamma functions Γ_1 and Γ_2, given by

$$\begin{aligned} \Gamma_1 &= i\left(\sum\nolimits_1 - \sum\nolimits_1^+\right) \quad \text{and} \\ \Gamma_2 &= i\left(\sum\nolimits_2 - \sum\nolimits_2^+\right). \end{aligned} \tag{18}$$

The self-energy terms affect the Hamiltonian in two ways. The real part of the self-energy term shifts the device eigenstates or energy level while the imaginary part of Σ causes the density of states to broaden while giving the eigenstates a finite lifetime. The electron density for the open system is now given by

$$[\rho] = \int_{-\infty}^{+\infty} [G^n(E)]\left(\frac{\mathrm{d}E}{2\pi}\right), \tag{19}$$

where $G^n(E)$ represents the electron density per unit energy and is given by

$$\begin{aligned} G^n(E) &= G(E)\sum\nolimits^{\text{in}}(E)G^+(E) \text{ where } \left[\sum\nolimits^{\text{in}}(E)\right] \\ &= \left[\Gamma_1(E)\right]f_1 + \left[\Gamma_2(E)\right]f_2. \end{aligned}$$

For plane wave basis functions, the current through the channel is calculated as the difference between the inflow and the outflow at any given contact,

$$I_j = -\frac{q}{\hbar}\int_{-\infty}^{+\infty} \text{trace}\left[\Gamma j A\right]f_1 - \text{trace}\left[\Gamma_j G^n\right], \tag{20}$$

where the subscript j indexes the contacts. For a two-terminal device $I_1 = -I_2$. The device examined in the present work is a double-gate MOSFET.

4.1 Phenomenological parameter η in NEGF formalism

The NEGF treatment of the junction side branches can be visualised by dealing with the floating probes in a similar way as the left and right contacts. Each probe can be viewed as connected with a reservoir with chemical potential $\mu_s(i)$, where i denotes the ith probe in the mesoscopic system. In general, the self-energy function Σ_s depend on the system density matrix and the Green function, which requires an iterative solution of the problem. Principally, the NEGF formalism provides clear descriptions on calculating Σ_s for each kind of scattering mechanism. However, we will not go into any of these models here. Instead, we will present results obtained from a phenomenological model that captures some of the important features of dissipative transport by a phenomenological parameter η, just like the phenomenological Büttiker probe coupling parameter ε, which is used for describing coupling strength of the scatterer and is related with the inelastic scattering rate. As the imaginary potential method gives the other way to describe the energy dissipation and the partially coherent transport, and because it modifies the Hamiltonian directly, it is more convenient to connect this method to the NEGF mechanisms. Based on the imaginary potential method [4], if we put one Büttiker probe in each mesh point, the scattering self-energy term will be

$$\sum\nolimits_s = -i\begin{bmatrix} \eta_1 & 0 & 0 & \cdots \\ 0 & \eta_2 & 0 & \cdots \\ 0 & 0 & \eta_3 & \cdots \\ \cdots & \cdots & \cdots & \cdots \end{bmatrix}, \tag{21}$$

where η is the phenomenological parameter, which is related with the inelastic scattering energy relaxation time by

$$\eta = \hbar/2\tau. \tag{22}$$

The device Green function then has the form,

$$G = [EI - H - \Sigma_1 - \Sigma_2 - \Sigma_s], \tag{23}$$

where Σ_1, Σ_2 and Σ_s denote the coupling with the left contact, right contact and the reservoir connected to Büttiker probe, respectively. As we have discussed about the imaginary potential method, Equation (23) gives the proper dynamic equation to study the dissipation processes inside the device.

4.2 Kinetic equations

The central part of the NEGF formalism is the kinetic equations, which relates the correlation function G^n and G^p with the scattering function Σ_{in} and Σ_{out}. The in-scattering function Σ_{in} states the rate at which electrons are scattered in the floating reservoir, and Σ_{out} states the rate at which holes are scattered in the floating reservoir or electrons are scattered out of it. They can be related with the scattering self-energy term Σ_s by the equation,

$$\Sigma_{\text{in}} = \left[F_s(\mu_s)\right]\cdot i\cdot\left[\Sigma_s - \Sigma_s^+\right] = \left[F_s(\mu_s)\right]\cdot\Gamma(E)$$
$$\Sigma_{\text{out}} = \left[1 - F_s(\mu_s)\right]\cdot i\cdot\left[\Sigma_s - \Sigma_s^+\right] = \left[1 - F_s(\mu_s)\right]\cdot\Gamma(E). \tag{24}$$

Here, we let each lattice site float to a thermal reservoir with a chemical potential μ_s different from each other, and $F_s(\mu_s)$ are the carrier distribution function with chemical potential μ_s. As we know that the Green function $G^R(r, r1)$ is the solution of the above equation with the source term equal to a delta function. For an arbitrary source function, the solution of Equation (24) has the form,

$$\psi(r) = \int G^R(r, r1)S(r1)\mathrm{d}r1. \tag{25}$$

Multiplying Equation (25) by the complex conjugate, we can have

$$\psi(r)\psi(r')^* = \int G^R(r,r1)G^R(r,r1')^* S(r)S(r1')^*\mathrm{d}r1\mathrm{d}r1'. \tag{26}$$

Noting that G^n represents the correlation between wave functions, and Σ_{in} represents the correlation between sources,

$$G^n(r, r')\sim\psi(r)\psi(r')^* \quad \Sigma_{\text{in}}(r1, r1')\sim S^R(r1, r1')^*, \tag{27}$$

we can write

$$G^n(r,r') = \int G^R(r,r1)\Sigma_{\text{in}}(r1,r1')G^A(r,r1')\mathrm{d}r1\mathrm{d}r1'. \tag{28}$$

In matrix notation, it will be $G^n = G^R\cdot\sum_{\text{in}}\cdot G^A$ which thus proves Equation (24).

The density matrix of the system can then be written as

$$2\pi[\rho(E)] = G^R\cdot(\Gamma_l + \Gamma_r)\cdot G^A + G^R\cdot\Sigma_{\text{in}}\cdot G^A$$
$$= F_l\cdot A_l + F_r\cdot A_r + F_S\cdot A_S.$$

The carrier density and the current can then be found from the density matrix in the above equation, where $F_{l,r,s}$ and $A_{l,r,s}$ are the Fermi distribution and spectral function for source, drain and each Büttiker probe. Thus, NEGF formalism gives us a sophisticated way to study the scattering behaviour inside the ultrascaled transistors.

5. Simulation of double-gate Si MOSFETs

The central problem for the simulation study to include the scattering processes is to determine the coupling strength of Büttiker probe or the phenomenological parameter η in the scattering self-energy term; η is the adjusting parameter, which means it can be found by comparing the simulation results with experimental observations. It should be pointed out that there are extra scattering processes for Si MOSFETs, comparing with a simple Si slab. For Si double-gate MOSFET, it will be helpful to get reasonable values of these parameters by studying the scattering processes considering the device configurations.

A lot of attention has been paid to two major scattering processes for Si MOSFETs scaled to $\sim$10 nm quasi-ballistic region. One is the surface roughness scattering of electrons at the Si/SiO_2 interface, and the other is the electron–electron scattering. Here, we will not have a detailed discussion on the scattering mechanisms. For a phenomenological modelling of the device behaviour in the inversion region, we will use the mobility mapping technique discussed in previous works [10–14]. The imaginary potential or the dephasing scattering self-energy term η can be related to the energy relaxation time by $\eta = \hbar/2\tau$ as shown in Equation (27). The energy relaxation time can be related with mobility by the equation [11],

$$\mu = q\tau/m^*. \tag{29}$$

So, we can approximately have

$$\eta\sim\hbar q/(2\mu m^*)\sim 0.003^*\left[\frac{\mu}{200}\cdot\frac{m^*}{m_e}\right]^{-1}\text{eV}. \tag{30}$$

Table 1 shows the relation between effective mobility and effective channel length for the measurement of real devices [10]. Although it is not accurate to get information from this table on the effective mobility value we are to use in our simulations due to the difference in fabrication details and device configurations, for a simple evaluation of the scattering effects on carrier transport in the $\sim$10 nm double-gate MOSFET, this table can give us some clue of the range of the mobility value we can put in our

Table 1. Measured μ_{eff} vs. L_{eff} relation for different E_{eff} [10].

S.No	μ_{eff} (cm^2/Vs)		Effective channel length (nm)
	E_{eff}(MV/cm) = 0.8	E_{eff}(MV/cm) = 1.1	
1	205	185	20
2	210	200	30
3	220	205	40
4	240	220	45
5	245	235	50
6	260	245	65
7	285	255	85

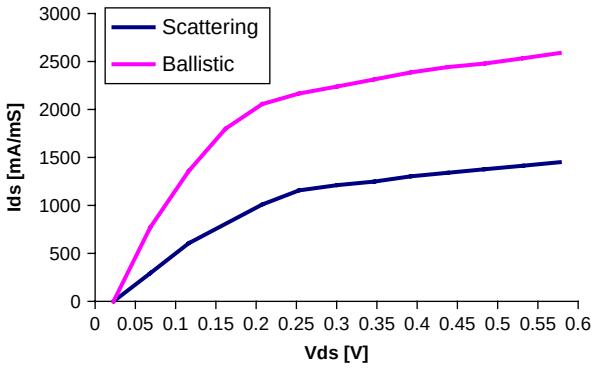

Figure 1. The simulation result includes scattering (blue), compared with the ballistic (pink) results. The device is the double-gate MOSFET with effective channel length of 10 nm, and the channel thickness is 7 nm, and oxide thickness for both top and bottom sides are 1.5 nm. The source–drain doping is 10^{20} cm^{-3}. The mapping mobility used in the simulation is 165 $cm^2/(Vs)$.

simulations. Here, we used the $\mu \sim 165\,cm^2/(Vs)$ for the transport dephasing calculations.

In Figure 1, we show our simulation results by the mobility mapping technique [12–14]. It is found that due to the scattering processes, the on current is reduced to ~54% of the ballistic current. It is just what is expected to see based on the increase of the on-state channel resistance. For generations, transistors are operating close to 50% of the ballistic current. The calculation results here show that the phenomenological model can give a reasonable evaluation of Si MOSFETs scaled to ~10 nm region.

6. Conclusion

Here, we reviewed and derived the quantum kinetic equations starting from the Hamiltonian of the electron--phonon system, and we also derived the self-energy functions for the electron--phonon interactions, which is found to be spatially local. As a result, we obtained the simplified quantum kinetic equations, which will constitute the basis of our study on the quantum transport in the semiconductor devices. We also introduced two kinds of expressions for the current density, and the linear response of the current in the near equilibrium condition. Finally, we introduced a simple double-gate MOSFET example, and applied the NEGF formalism to obtain the analytic expressions for the retarded Green function and the other physical quantities.

References

[1] R.C. Ashoori, *Electrons in artificial atoms*, Nature 379 (1996), pp. 413–419.
[2] R. de Picciotto, H.L. Stormer, L.N. Pfeiffer, K.W. Baldwin, and K.W. West, *Four-terminal resistance of a ballistic quantum wire*, Nature 411 (2001), pp. 51–54.
[3] D.K. Ferry and S.M. Goodnick, *Transport in Nano Structure*, Cambridge University Press, Cambridge, 1997.
[4] G. Grosso and G.P. Parravicini, *Solid State Physics*, Academic Press, New York, 2000.
[5] A.L. Fetter and J.D. Walecka, *Quantum Theory of Many-Particle System*, McGraw-Hill, New York, 1971.
[6] C. Jacoboni and L. Reggiani, *The Monte Carlo method for the solution of charge transport in semiconductors with applications to covalent materials*, Rev. Modern Phys. 55(3) (1983), pp. 645–705.
[7] G.D. Mahan, *Many-Particle Physics*, 2nd ed., Plenum Press, New York, 1990.
[8] J. Bardeen and W. Shockley, *Deformation potentials and mobilities in nonpolar crystals*, Phys. Rev. 80(1) (1950), pp. 72–80.
[9] A. Szafer and A.D. Stone, *Theory of quantum conduction through a constriction*, Phys. Rev. Lett. 62(3) (1989), pp. 300–303.
[10] S. Takagi, A. Toriumi, M. Iwase, and H. Tango, *On the universality of inversion layer mobility in Si MOSFET's: Part I-effects of substrate impurity concentration*, IEEE Trans. Electron Dev. 41(12) (1994), pp. 2357–2362.
[11] A. Rahman and M.S. Lundstrom, *A compact scattering model for the nanoscale double-gate MOSFET*, IEEE Trans. Electron Dev. 49(3) (2002), pp. 481–489.
[12] W. Hansch et al., *Carrier Transport Near the Si/SO_2 Interface of a MOSFET*, Solid State Electron. 32(10) (1989), pp. 839–849.
[13] A. Svizhenko, M.P. Anantram, T.R. Govindan, B. Biegel, and R. Venugopal, *Two-dimensional quantum mechanical modeling of nanotransistors*, J. Appl. Phys. 91 (2002), pp. 2343–2354.
[14] U. Landman, R.N. Barnett, A.G. Scherbakov, and P. Avouris, *Metal-semiconductor nanocontacts: silicon nanowires*, Phys. Rev. Lett. 85(9) (2000), pp. 1958–1961.